

Lawrence Berkeley National Laboratory

Recent Work

Title

HIGH ENERGY X-RAY RESPONSE OF PHOTOGRAPHIC FILMS. MODELS AND MEASUREMENTS

Permalink

<https://escholarship.org/uc/item/6tf1m8jb>

Author

Henke, B.L.

Publication Date

1986-05-01



Lawrence Berkeley Laboratory

UNIVERSITY OF CALIFORNIA

RECEIVED
LAWRENCE
BERKELEY LABORATORY

Accelerator & Fusion Research Division

OCT 13 1986

LIBRARY AND
DOCUMENTS SECTION

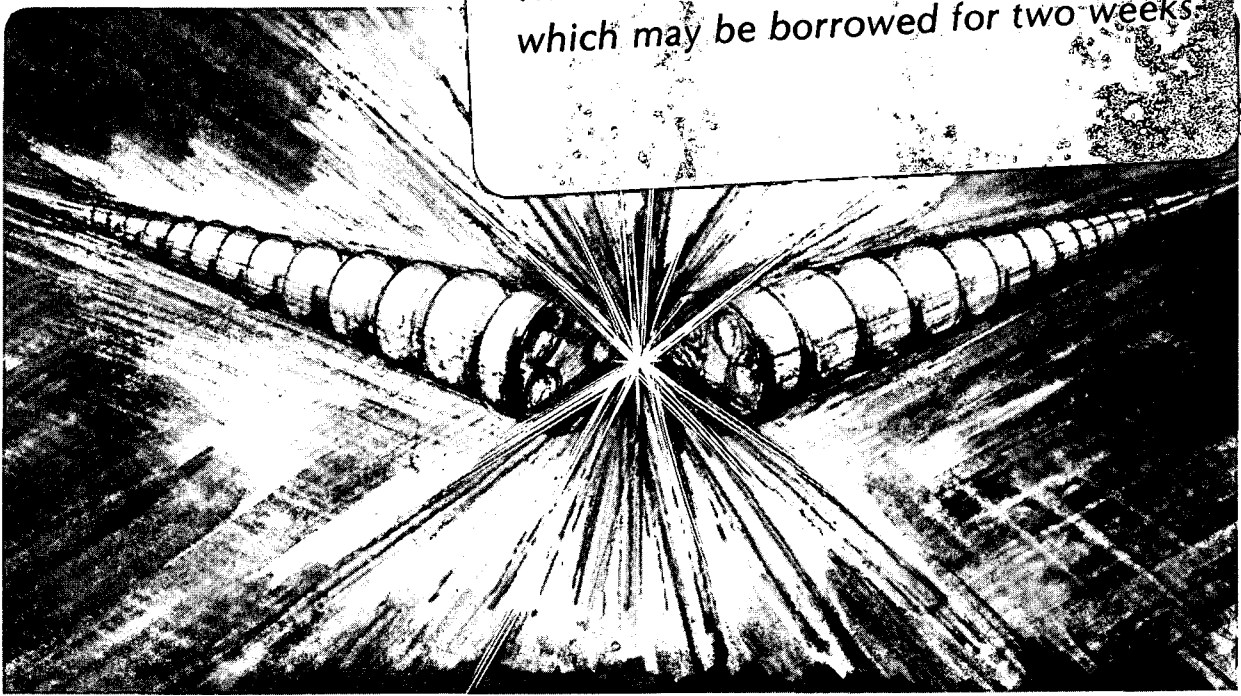
Submitted to Journal of the Optical Society of
America

HIGH ENERGY X-RAY RESPONSE OF PHOTOGRAPHIC FILMS.
MODELS AND MEASUREMENTS

B.L. Henke, J.Y. Uejio, G.F. Stone,
C.H. Dittmore, and F.G. Fujiwara

May 1986

TWO-WEEK LOAN COPY
*This is a Library Circulating Copy
which may be borrowed for two weeks.*



LBL-21564
c.2

DISCLAIMER

This document was prepared as an account of work sponsored by the United States Government. While this document is believed to contain correct information, neither the United States Government nor any agency thereof, nor the Regents of the University of California, nor any of their employees, makes any warranty, express or implied, or assumes any legal responsibility for the accuracy, completeness, or usefulness of any information, apparatus, product, or process disclosed, or represents that its use would not infringe privately owned rights. Reference herein to any specific commercial product, process, or service by its trade name, trademark, manufacturer, or otherwise, does not necessarily constitute or imply its endorsement, recommendation, or favoring by the United States Government or any agency thereof, or the Regents of the University of California. The views and opinions of authors expressed herein do not necessarily state or reflect those of the United States Government or any agency thereof or the Regents of the University of California.

HIGH ENERGY X-RAY RESPONSE OF PHOTOGRAPHIC FILMS.
MODELS AND MEASUREMENTS*

B.L. Henke and J.Y. Uejio
Lawrence Berkeley Laboratory
University of California
Berkeley, California 94720

G.F. Stone and C.H. Dittmore
Lawrence Livermore National Laboratory
Livermore, California 94550

F.G. Fujiwara
University of Hawaii
Honolulu, Hawaii 96822

ABSTRACT

A detailed characterization has been established for the new, high sensitivity double-emulsion Kodak Direct Exposure Film (DEF). The experimental data base consisted of density-vs-exposure measurements that were duplicated at several laboratories for x-radiations in the 1000-10,000 eV region. The absorption and geometric properties of the film were determined which, along with the density-exposure data, allowed the application of a relatively simple analytical model description for the optical density, D , as a function of the intensity, I (photons/ μm^2), the photon energy, E (eV) and the angle of incidence, θ , of the exposing radiation. A detailed table is presented for the I values corresponding to optical densities in the 0.2-2.0 range and to photon energies, E (eV), in the 1000-10,000 eV region. Experimentally derived conversion relations have been obtained which allow the density values to be expressed as either diffuse or specular. Also presented here is a similar characterization of the complementary, single-emulsion x-ray film, Kodak SB-5 (or 392). For the 1000-10,000 eV region this x-ray film is appreciably less sensitive but with higher resolution.

*Submitted to the Journal of the Optical Society of America, B (May, 1986)

I. INTRODUCTION

There is a considerable need at this time for absolute, high sensitivity, position-sensitive x-ray detection for imaging and for spectroscopic analysis in the higher x-ray photon energy region of 1000-10,000 eV. An important example of such a need is that for the absolute x-ray diagnostics of high temperature plasmas which are involved in fusion energy and x-ray laser research. For many such applications, position-sensitive x-ray detection with photographic films can be exceptionally simple and effective¹.

In companion works^{2,3} we have recently reported the development of effective two-parameter analytical equations for the optical density, D , that is generated in thick and thin single-emulsion films by x-radiation in the 100-1000 eV region. These equations are functions of the exposure, I (photons/ μm^2), the photon energy, E (eV), and of the angle of incidence, θ . We have applied these model relations to obtain detailed characterizations for the response of the Kodak films that are currently used for position-sensitive detection in the low energy x-ray region, viz. Kodak 101, RAR 2492, 2495 and 2497, and SB-392. In the present work, we extend this analytical modeling to obtain the detailed response characteristics of the double-emulsion films, and specifically of the Kodak Direct Exposure Film, DEF, which has been designed for high sensitivity at the higher photon energies (1000-10,000 eV) as compared to that of its predecessor, the Kodak No-Screen double-emulsion film which is no longer manufactured. We have also extended by a similar procedure the characterization of the complementary, single-emulsion x-ray film, the Kodak SB-5 (or 392) for this higher photon energy region.

II. ANALYTICAL MODELS FOR PHOTOGRAPHIC FILM RESPONSE

In Ref. 2 we have developed a phenomenological model for the photographic response of thick emulsions which implicitly expresses the photon energy dependence through the linear absorption coefficients for the x-ray absorption within a supercoat, for the heterogeneous absorption within the emulsion, and for the absorption within a AgBr film grain. This model led to a "universal" function, ϕ , for the density, D , as a function of exposure, I , defined as

$$\alpha D = \phi(\beta I) \quad (1)$$

where α and β are the photon energy dependent factors given by

$$\alpha = \mu' / \sin \theta \quad (2)$$

$$\text{and } \beta = [1 - \exp(-\mu_1 d)] \exp(-\mu_0 t_0 / \sin \theta) \quad (3)$$

Note: In Ref. 2, α was defined as $(\frac{\sin \theta}{\mu'} + d_0)^{-1}$ where d_0 is a measure of the thickness of the first layer of AgBr grains which may be the primary absorption layer for the low photon energies (< 1000 eV). This parameter, d_0 , can be neglected for the higher photon energies of interest here.

These "universalizing" factors, α and β , are expressed in terms of the energy dependent linear absorption coefficients, μ_0 , μ_1 , and μ' , for respectively the supercoat, the film grain material, AgBr, and for the heterogeneous emulsion of these grains within gelatin. The geometric parameters that have been chosen here to define an emulsion are the supercoat thickness, t_0 , the emulsion thickness, T , and the effective film grain thickness, d . The angle of incidence, θ , of the exposing radiation is measured from the film plane.

An example of the predicted universal curve, $\alpha D = \phi(\beta I)$, will be presented below using measured D-I data for the DEF film.

It was also predicted and demonstrated (see Refs. 2 and 3) that this universal curve may be efficiently fit by a two-parameter equation for the thick (completely absorbing) emulsion response, viz.:

$$\alpha D = a \ln(1 + b\beta I) \quad (4)$$

The parameters, a and b , may be determined by least squares fitting of the experimentally determined and universally plotted data.

For the corresponding response of a thin (incompletely absorbing) emulsion of thickness, T , we must subtract from the optical density, D , given by (4) for the infinitely thick emulsion, the contribution of that density that is generated within the layers below a depth, T , (where the exposing intensity at the emulsion's top surface has been reduced by the factor, $\exp(-\mu' T / \sin \theta)$). This consideration leads immediately to the simple modification of (4) for the thin-emulsion response, viz.

$$\alpha D = a \ln \left[\frac{1 + b\beta I}{1 + b\beta I \exp(-\mu' T / \sin \theta)} \right] \quad (5)$$

We now extend this model description for the double-emulsion film. In Figs. 1 and 2 we describe the properties of a double-emulsion film (presented here for the new DEF film). For such a film with photon energies above about 4000 eV a significant amount of additional optical

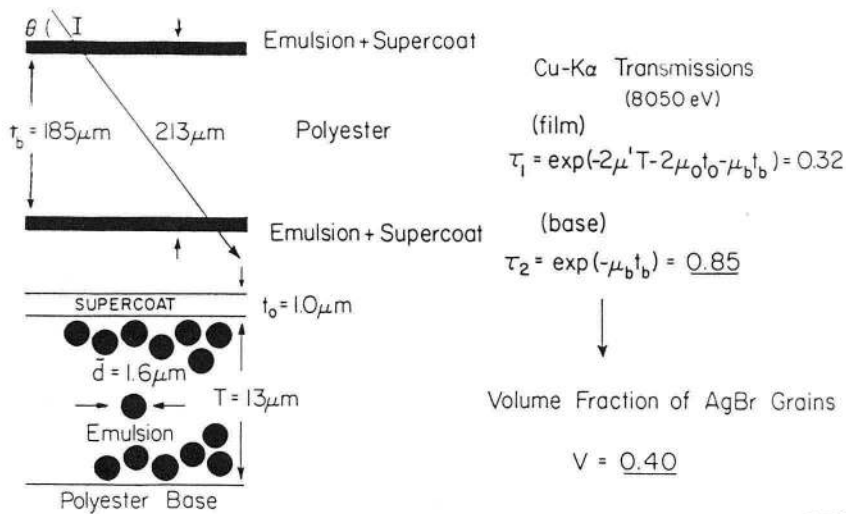
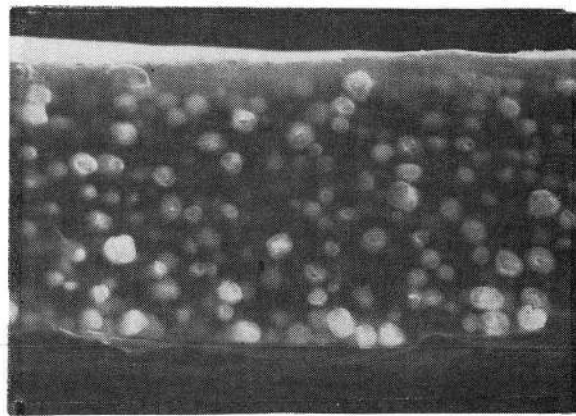


Fig. 1. Properties of the double-emulsion film, DEF. The micrometered total thickness and the transmissions for Cu-K α (8050 eV) of the film and of the polyester base yield the indicated values of the emulsion and base thicknesses, T and t_b , and of the volume fraction of the AgBr grains, V. (For the base transmission measurements, the emulsions are dissolved away using a bleach solution.) The estimate of the film grain size, d, is obtained from SEM film cross section photos as that shown in Fig. 2. The supercoat thickness, t_0 , is sensitively determined by model equation fitting of the low energy x-ray exposure data.

Fig. 2. Cross section of a DEF emulsion, imaged by a scanning electron microscope. Sample sections were obtained by breaking liquid-nitrogen frozen pieces of film. The average grain size was estimated from such photos by the measurement of the outermost, imbedded grains.

SEM Image of DEF

← 5 μ m →



Polyester Base

density will be generated within the second emulsion. This second thin emulsion section will contribute a density that may be predicted by an expression like that described by the model relation (5) for a thin emulsion but with two simple modifications--we replace in (5) the term for the supercoat transmission, $\exp(-\mu_0 t_0 / \sin \theta)$ (in the β factor) by $\exp(-\mu_b t_b / \sin \theta)$ with μ_b and t_b the linear absorption coefficient and the thickness of the polyester base, and we replace the incident intensity, I in (5) by its reduced value at the top surface of the polyester base, $I \exp(-\mu_0 t_0 - \mu' T)$. In terms of our originally defined value of β given in (3), the additional density, ΔD , within the second emulsion may then be deduced directly from (5) to be:

$$\alpha \Delta D = \ln \left(\frac{1 + \beta I \exp [(-\mu_b t_b - \mu' T) / \sin \theta]}{1 + \beta I \exp [(-\mu_b t_b - 2\mu' T) / \sin \theta]} \right) \quad (6)$$

In Ref. 2 we have discussed the justification for a linear addition of the optical density contributions of successive layers when the total optical density is within the usual range of density measurements. With the same assumption, we then add the ΔD density given by (6) to that of

the upper thin-emulsion contribution given by (5) to obtain the expression for the double-emulsion response, viz.:

$$D = a \ln \left[\left(\frac{1+b\beta I}{1+b\beta I \exp\{(-\mu' T)/\sin \theta\}} \right) \left(\frac{1+b\beta I \exp\{(-\mu_b \tau_b - \mu' T)/\sin \theta\}}{1+b\beta I \exp\{(-\mu_b \tau_b - 2\mu' T)/\sin \theta\}} \right) \right] \quad (7)$$

It should be noted that the fitting parameters a and b , appearing in the above Eqs. 4 through 7 for the thick, thin, and double-emulsion films are those initially suggested for the universal curve fitting and thus for the thick emulsion, low energy photon absorption regime. These same values of a and b then reappear, as described above, in the subsequently developed expressions for the thin and double-emulsion, higher energy photon absorption regime--with the important assumption that these parameters will be independent of photon energy. For the photon energies in the 100-10,000 eV region this assumption is considered to be a good one because (1) these photon energies are sufficiently high to ensure that a film grain is rendered developable by a single photon absorption, and (2) these photon energies are sufficiently low to ensure that any additional excitation of grains by high energy photoelectrons is negligible.

III. CHARACTERIZATION OF THE KODAK DEF FILM

We would like to develop here a detailed characterization of the Kodak DEF double-emulsion film using the model relations presented above and experimental density-vs-exposure (D-I) data that has been obtained independently at four laboratories for the 1000-10,000 eV region. In all of these investigations, the films were processed with conventional, x-ray developers for microdensitometric applications. These studies may be described as follows:

- (1) Phillips and Phillips (1985)⁴ - Cu-K α (8050 eV); developed with agitation in GBX for 3 min at 68°F; and densitometered with an Optronics-1000 using matched influx and efflux optics of 0.25 N.A.
- (2) Rockett et al (1985)⁵; Cu-L α (930 eV), Al-K α (1490 eV), Si-K α (1740 eV), Ti-K α, β (4510-4930 eV) and Co-K α (6930 eV); developed with agitation in Kodak Industrex for 5 min at 68°F; and densitometered with a Macbeth Transmission Densitometer, TD-404 (diffuse density): and
- (3) Henke, et al, this work; Cu-L α (930 eV), Al-K α (1490 eV) and Cu-K α (8050 eV); developed with agitation in Kodak Rapid X-Ray (RXR) for 6 min at 72°F; and densitometered with a PDS Microdensitometer using matched influx and efflux optics of 0.1 N.A.

All exposure data were for normal incidence radiation ($\sin \theta = 1$). For these measurements it is important to have highly monochromatized exposing radiation of accurately known intensity. The Phillips and

Phillips⁴ Cu-K α radiation, from a copper anode, was Ni foil filtered, focussed by a double mirror reflection and Bragg diffracted from a polyethylene sample. The Rockett et al⁴ characteristic line radiations from x-ray tube anodes were filtered and the background continuum radiation was estimated by pulse-height analysis with their flow proportional and solid state x-ray detectors. In this work, we have applied the characteristic x-ray line radiations from a demountable anode source which are then filtered and Bragg reflected onto a normal incidence detection circle of an elliptically curved crystal analyzer spectrograph.^{3,6} (See Fig. 3.) An intensity spectrum is obtained by scanning an absolutely calibrated flow proportional counter along this detection circle. Photographic spectra are then obtained for a series of different exposures of the 35 mm film that is transported along the same detection circle. Microdensitometry is with an effective slit of dimensions that match those of the proportional counter slit window and of width smaller than that of the diffraction line spectrum widths. At the monoenergetic Bragg diffraction line peaks, the net optical densities, D , in the photographic spectra are related to the corresponding intensity peaks, I (photons/ μm^2) in the intensity spectra. (This "operational" procedure for film calibration was designed to correspond precisely to the actual procedure, in reverse, for obtaining absolute measurements of intensities from photographic spectra.)

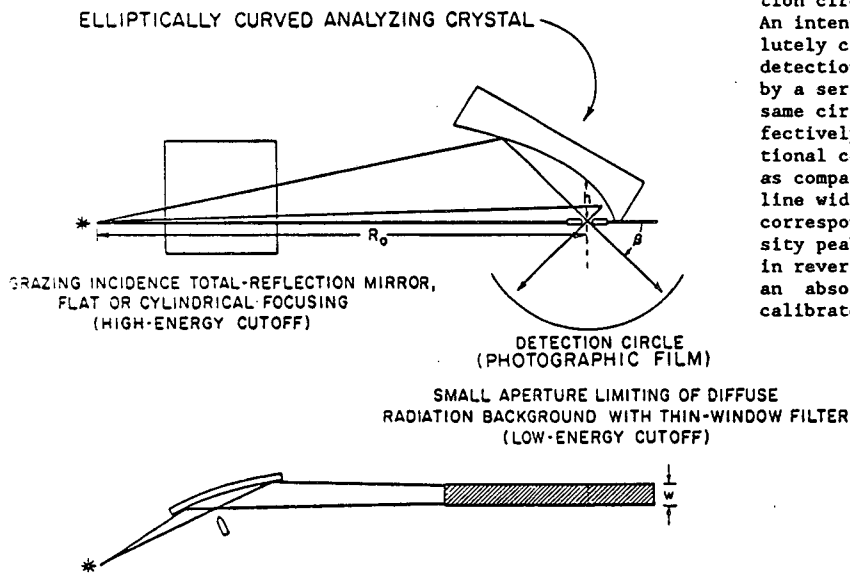


Fig. 3. Method for obtaining monoenergetic, characteristic line exposures, normally incident to a detection circle of an elliptical analyzer spectrograph. An intensity spectrum is obtained by scanning an absolutely calibrated flow proportional counter along this detection circle. Photographic spectra are obtained by a series of exposures of film transported along the same circle. Microdensitometry is with a slit of effectively the same dimensions as that of the proportional counter slit window and of width that is small as compared to the instrumental broadened diffraction line width. The density-exposure data are taken from corresponding photographic density and absolute intensity peaks (photons/ μm^2), operationally similar, but in reverse, to the procedure for the determination of an absolute intensity of spectral lines from a calibrated photographic film spectrum.

A. Normalizing Independent D-I Data Sets

In our combining of the DEF calibration data from the independent laboratory measurements described above, we consider that batch-to-batch variations and any others that result from using different (but conventional) x-ray film development procedures can be assumed to be small as compared to the variations resulting from density/intensity measurement errors. All density values are for net density, i.e., that above the unexposed developed film background density. We ensure that this background correction has been precisely accomplished by requiring that a linear plot of D vs I for the lower densities does indeed extrapolate to the 0-0 origin.

Before combining these data for fitting by our model relations, we converted the D-I data of Phillips and Phillips⁴ to an equivalent 5 min development result using their D vs time of development curves (a small correction). We then converted all of the D-I data of Refs. 4 and 5 to the specular density values at 0.1 N.A. for the influx and efflux microdensitometer optics. This is a straightforward conversion procedure because the factors, D_s/D_d (net specular density/net diffuse density), needed for this conversion are slowly varying functions of diffuse density, D_d , and are independent of the photon energy³. We have measured the D_s/D_d vs D_d curves which are shown in Fig. 4 for D_s at 0.1 and 0.25 N.A. (using the PDS and the Macbeth (double-diffuse) densitometers).

By fitting these D_s/D_d data, we obtain the required conversion equations:

$$D_{0.1}/D_d = 1.9 - 0.35 D_d + 0.092 D_d^2 \quad (8)$$

$$\text{and } D_{0.25}/D_d = 1.31$$

which yield,

$$D_{0.1}/D_{0.25} = 1.5 - 0.20 D_{0.25} + 0.041 D_{0.25}^2 \quad (9)$$

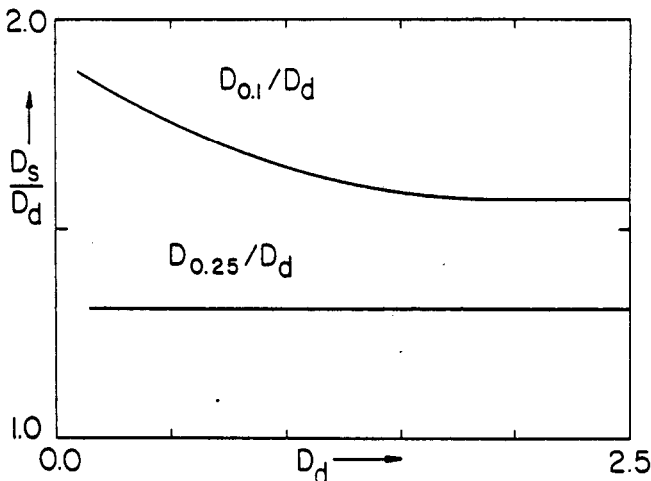


Fig. 4. Plots of experimentally measured conversion ratios, D_s/D_d (net specular density/net diffuse density) vs diffuse D_d for specular density measurements with matched influx-efflux optics at 0.1 and 0.25 N.A. and for total diffuse density. (These ratios are essentially independent of photon energy and are for the conventional, x-ray film development.) These experimental curves yield the conversion equations (8) and (9) that have been applied here to normalize the data sets of Refs. 4 and 5.

B. Fitting the Model Equations

The linear absorption coefficients, μ_0 , μ_1 , μ' and μ_b for an assumed gelatin supercoat ($C_8H_{16}O_5N_2$, $\rho = 1.40 \text{ gm/cm}^3$), for AgBr, for the heterogeneous emulsion and for the polyester base ($C_5H_4O_2$, $\rho = 1.40 \text{ gm/cm}^3$), respectively, were determined as described in the companion Refs. 2 and 3, using photoabsorption data compiled by Henke, et al⁷.

Note: We have been unable to obtain from the manufacturer of the DEF film the chemical formula for their special supercoat material and we assume here that its linear absorption coefficient is essentially proportional to that for gelatin and that, for example, a difference in mass density can be accommodated in our choice of an effective value for the supercoat thickness, t_0 , determined by a precise fitting of the measured lower photon energy data. Similarly, the geometric specifications for the DEF film are not available and we have therefore developed the following procedure for their determination:

The total DEF film thickness was carefully micrometered to yield a value of about 213 μm . We then measured the x-ray transmission of the base-plus-emulsion choosing an x-ray wavelength that is transmitting in the 20%-40% range and with a negligible absorption within the thin supercoat. This transmission is given as τ_1 in Fig. 1. The emulsion is then dissolved away from the polyester base by soaking for about ten minutes in a 1:1 dilution of a common bleach solution (5% aqueous solution of sodium hypochlorite, by weight). The transmission, defined in Fig. 1 as τ_2 for the remaining polyester base, is then measured. We have chosen the $\text{Cu-K}\alpha$ (8050 eV) line radiation for these transmission measurements, derived from a Cu anode, filtered and Bragg reflected with a PET crystal analyzer. The values for τ_1 and τ_2 are presented in Fig. 1 for the DEF film and were 0.32 and 0.85 respectively. These results along with that for the film thickness yielded the values of 13 μm and 185 μm for the emulsion and polyester base thicknesses and a volume fraction, V , of the AgBr grains equal to 0.40. The general relations for this determination of the emulsion and base thicknesses follow from the transmission equations in Fig. 1 and are:

$$T = (1/\mu') \ln \sqrt{\tau_2/\tau_1} \quad (10)$$

and

$$t_b = (1/\mu_b) \ln(1/\tau_2) \quad (11)$$

in which μ' , the linear heterogeneous emulsion absorption coefficient, contains the dependence upon the volume fraction, V (See Ref. 2).

The film grain size was estimated from averaged measurements of the outermost imbedded grains imaged in scanning electron microscope micrographs of the DEF film cross section. The SEM photos were obtained by Dixon⁸ using small DEF sections obtained by breaking liquid-nitrogen frozen pieces of the DEF film. An example of one of these micrographs was shown in Fig. 2. As will be demonstrated below, our model relation (7) requires only an estimate of the effective grain size. We have

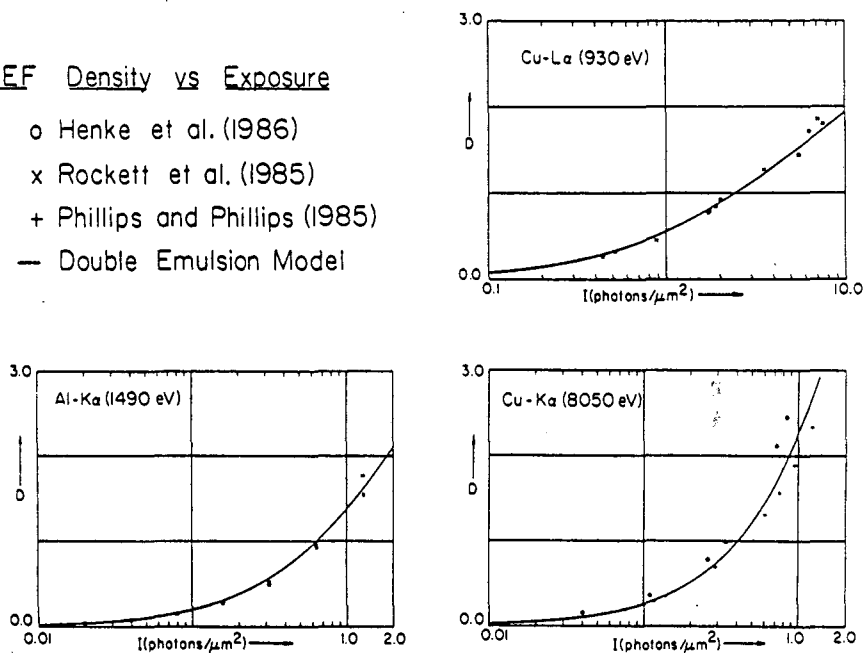
determined from the SEM photos the average grain size, d , to be about $1.6 \mu\text{m}$. It is not feasible to determine an accurate value of the supercoat thickness, t_0 , from these SEM photos. We therefore establish this value along with those of the fitting parameters, a and b , by a least squares "best" fitting of the model equation (7) to the D-I data sets. Fitting only the duplicated data sets that are plotted in Fig. 5 (from four laboratories), we obtain the following values for the DEF film:

$$a = 0.680 \mu\text{m}^{-1}, b = 1.69 \mu\text{m}^2 \text{ and } t_0 = 1.0 \mu\text{m}$$

DEF Density vs Exposure

- o Henke et al. (1986)
- x Rockett et al. (1985)
- + Phillips and Phillips (1985)
- Double Emulsion Model

Fig. 5. The density-exposure data chosen here for the model equation fitting, consisting of independent, duplicated measurements of several laboratories at the representative photon energies, Cu-L α (930 eV), Al-K α (1490 eV) and Cu-K α (8050 eV). Also plotted here are the predicted D-I curves obtained by fitting the analytical model relation (7) to these data. Optical densities are net densities (above non-exposed developed background density) as would be measured by microdensitometry using matched influx-efflux optics of 0.1 N.A.



Our determinations of the geometric parameters that are needed in the model relation (7) are in excellent agreement with those that have been independently determined by Rockett et al⁵ upon another DEF film batch.

In Fig. 6 we present our model D-I curves along with the unduplicated experimental data of Rockett et al⁵ for Si-K α (1740 eV), Ti-K α, β (4510 eV, 4930 eV) and Co-K α (6930 eV) which were not included in the data base (presented in Fig. 5) chosen for our fitting of (7). Our prediction of their D-I curve for 1740 eV is excellent. We do not agree, however, with their D-I measurements at the higher photon energies, 4510/4930 eV and 6930 eV. Only for these energies have they replaced their proportional gas counter detector by a Si(Li) solid state detector. A possible explanation for their higher density values at

DEF Density vs Exposure

x Rockett et al.

— Double Emulsion Model

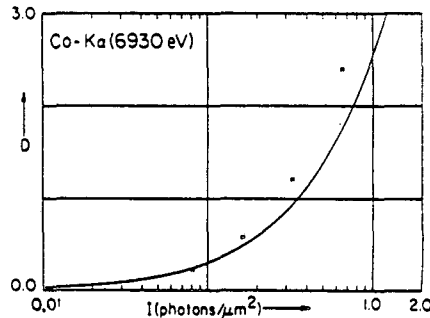
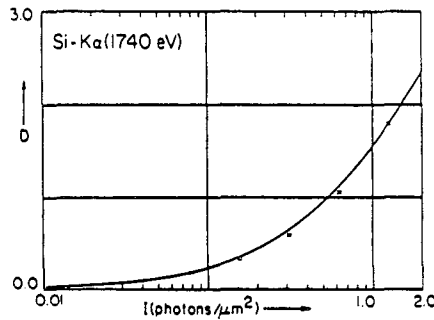
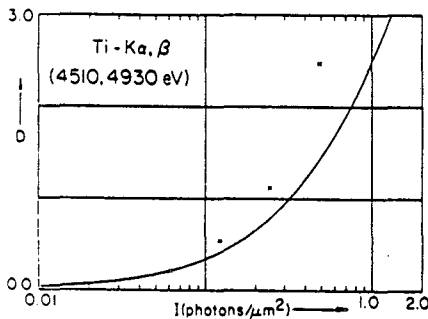


Fig. 6. Applying the model equation (7) determined by the data sets shown in Fig. 5 to predict D-I curves for additional but unduplicated D-I data at photon energies, Si-K α (1740 eV), Ti-K α,β (4510, 4930 eV) and Co-K α (6930 eV). The prediction for the photon energy at 1740 eV is excellent. It is suggested here that the high density values shown here for measurements with Ti-K α and Co-K α radiations are excessively high because the films were also exposed to the appreciably higher continuum radiation that cannot be completely filtered out at the higher photon energies and which was not completely included in the detector "window". (A Si(LI) solid state detector was used only for these two radiations). See Ref. 5

these higher photon energies is that the film exposure included that for the higher continuum background associated with these energies (not eliminated in their filtered, direct source radiation and which may not have been completely included in their solid-state detector "window"). Our rejection of these two data sets in our fitting of (7) seems to be strongly justified by the very satisfactory, simultaneous fitting of the lower energy data along with that for the highest photon energy, 8050 eV, (obtained by Phillips and Phillips⁴ and by this work).

To demonstrate the "universality" of this model description for the DEF film we present in Fig. 7 the universal plot, $\alpha D = \phi(\beta I)$, using only the D-I data sets for the x-radiations that are essentially completely absorbed within the first emulsion, viz. Cu-L α (930 eV), Al-K α (1490 eV) and Si-K α (1740 eV) along with the model fit curve for a thick emulsion (4) using the geometric parameters and values of \underline{a} and \underline{b} as presented above for the overall fit of (7) for the DEF film at both the low and the high photon energies.

It was noted earlier that the grain size, d , chosen here to be $1.6 \mu\text{m}$, was not amenable to direct, accurate evaluation, but, nevertheless, was not required to be known accurately in our model description (7). The fitting parameter, \underline{b} , can compensate for a variation in d , (from (3), we note that $b\beta \approx b \mu_1 d$ for the higher photon energy dependence upon d in the model equations). To illustrate this insensitivity, we plot in Fig. 8 the intensity I (photons/ μm^2) that is required to generate an optical specular density, $D_{0.1}$, of 0.5, as a function of the photon energy, E (eV), using the "best choice parameters"

Fig. 7. Demonstration of the universality of the plot of the αD vs βI data for the x-radiations that are completely absorbed within the first emulsion, Cu-L α (930 eV), Al-K α (1490 eV) and Si-K α (1740 eV) (for the data by Rockett et al. (X) and Henke et al (O) shown in Figs. 4 and 5). Also plotted here is the model relation (4) using parameters derived by fitting data at both the high and the low energies.

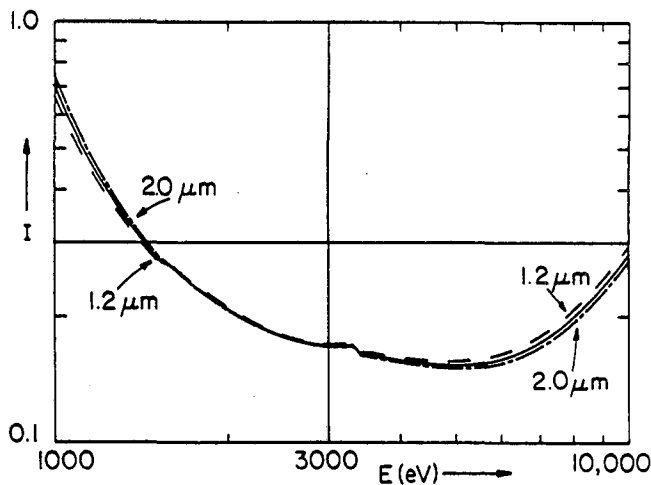
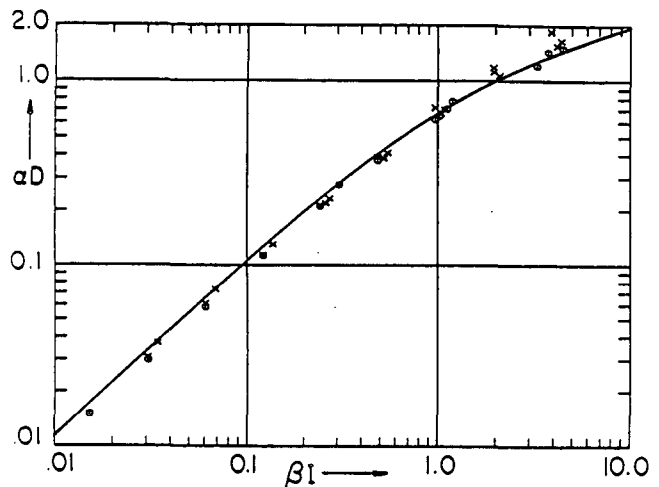


Fig. 8. Plotted here for the DEF film is the intensity, I (photons/ μm^2) that is required to generate a specular density, $D_{0.1} = 0.5$ vs photon energy, E (eV), using the "best" fit model curve (7) for the data sets shown in Fig. 5 and the parameters listed in Fig. 1 with the AgBr grain size at the $1.6\mu\text{m}$ and also at the varied values of $1.2\mu\text{m}$ and $2.0\mu\text{m}$ in order to illustrate the insensitivity of (7) to the film grain size. (The fitting parameter, b , effectively compensates for a variation in d .)

determined above (and listed in Fig. 1), along with similar best fit intensity curves with the grain size parameter, d , varied from the chosen value $1.6\mu\text{m}$ to the values 1.2 and $2.0\mu\text{m}$.

C. Expressing the Detailed Photographic Response of the DEF Film

In Fig. 9 we present the sensitivity of the DEF film for the 1000-10,000 eV region, defined here as the reciprocal of that intensity (photons/ μm^2) which is required to generate an optical density, $D_{0.1}$, of 0.5. Also shown here is the same sensitivity curve calculated for the first emulsion only (effect of second emulsion removed) in order to illustrate for what photon energies there is a significant improvement resulting from having the double emulsion. In Fig. 10 we present this DEF film sensitivity curve for the 1000-10,000 eV and compare it to that for the single-emulsion x-ray film Kodak SB-392 (characterized for this high energy region as described in Sec. IV).

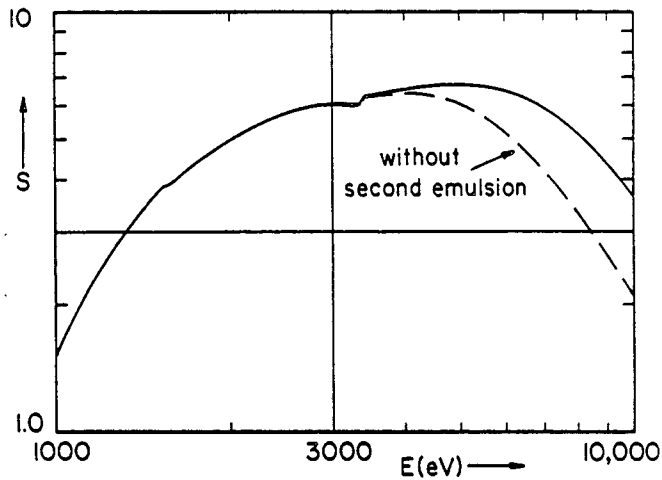
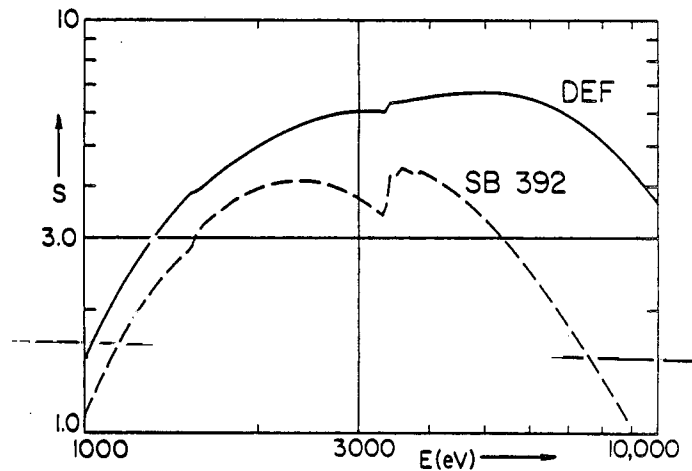


Fig. 9. The sensitivity, S , for the DEF film in the 1000-10,000 eV region. S is defined here as the reciprocal of the intensity that is required to generate an optical density, $D_{0.1} = 0.5$. Also shown is the calculated sensitivity, S , for the first emulsion only in DEF in order to illustrate the significant improvement in the DEF sensitivity for photon energies higher than about 4000 eV.

Fig. 10. The sensitivity, S , is plotted here for an optical density, $D_{0.1} = 0.5$ and for the 1000-10,000 eV region for DEF and compared to that sensitivity for the single-emulsion film Kodak SB-392 (as characterized in Sec. IV below).



In Table 1, we present for Kodak DEF a detailed tabulation, using the fitted model relation (7), for the normal incidence intensity I (photons/ μm^2) which corresponds to a given specular optical density, $D_{0.1}$, (microdensitometered at matched 0.1 N.A. optics) in the 0.2-2.0 range, and at a given photon energy, E (eV), in the 1000-10,000 eV region. Corresponding values of diffuse optical densities and those microdensitometered at matched 0.25 N.A. optics for this Table 1 can be obtained by using the conversion relations (8) and (9).

IV. CHARACTERIZATION OF THE KODAK SB-392

For optimized measurements with position-sensitive photographic detection, higher resolution may be more important than higher sensitivity. Then the alternative single-emulsion x-ray film, Kodak SB-5 or SB-392 film should be considered. (SB-5 and SB-392 differ only in format, i.e. sheet or 35 mm respectively.) In Ref. 3 we presented a characterization of the SB-392 specifically for the low energy x-ray

Table 1: Exposure [photons/cm²] vs Net Optical Density, D - Normal Incidence and Photon Energy, E(eV) for the Kodak SB-32

Photon Energy E(eV)	Net Density, D (Specular, 0.1 x 0.1 N.A.)										Wavelength λ(Å)
	0.2	0.4	0.6	0.8	1.0	1.2	1.4	1.6	1.8	2.0	
1000	2.24-01	5.03-01	6.50-01	1.28-00	1.82-00	2.49-00	3.32-00	4.36-00	5.65-00	7.26-00	12.40
1050	1.95-01	4.36-01	7.29-01	1.09-00	1.53-00	2.07-00	2.73-00	3.54-00	4.54-00	5.75-00	11.81
1100	1.74-01	3.84-01	6.39-01	9.44-01	1.31-00	1.76-00	2.30-00	2.95-00	3.74-00	4.69-00	11.27
1150	1.57-01	3.44-01	5.67-01	8.33-01	1.15-00	1.53-00	1.98-00	2.52-00	3.17-00	3.84-00	10.78
1200	1.43-01	3.12-01	5.11-01	7.46-01	1.02-00	1.35-00	1.74-00	2.20-00	2.73-00	3.37-00	10.33
1250	1.32-01	2.86-01	4.66-01	6.76-01	9.22-01	1.21-00	1.55-00	1.94-00	2.40-00	2.94-00	9.92
1300	1.22-01	2.64-01	4.29-01	6.19-01	8.40-01	1.10-00	1.39-00	1.74-00	2.14-00	2.60-00	9.54
1350	1.14-01	2.46-01	3.98-01	5.72-01	7.72-01	1.00-00	1.27-00	1.57-00	1.82-00	2.33-00	9.18
1400	1.08-01	2.31-01	3.72-01	5.33-01	7.15-01	9.25-01	1.17-00	1.44-00	1.75-00	2.11-00	8.86
1450	1.02-01	2.19-01	3.50-01	5.00-01	6.69-01	8.61-01	1.08-00	1.33-00	1.61-00	1.93-00	8.55
1500	9.76-02	2.08-01	3.32-01	4.71-01	6.29-01	8.07-01	1.01-00	1.23-00	1.49-00	1.78-00	8.27
1600	8.10-02	1.72-01	2.73-01	3.87-01	5.15-01	6.58-01	8.19-01	9.99-01	1.20-00	1.43-00	6.89
1800	7.73-02	1.64-01	2.60-01	3.67-01	4.86-01	6.19-01	7.68-01	9.34-01	1.12-00	1.33-00	6.53
2000	7.42-02	1.57-01	2.48-01	3.49-01	4.61-01	5.86-01	7.24-01	8.78-01	1.05-00	1.24-00	6.20
2100	7.17-02	1.51-01	2.38-01	3.34-01	4.40-01	5.59-01	6.87-01	8.30-01	9.89-01	1.16-00	5.80
2200	6.86-02	1.46-01	2.30-01	3.22-01	4.23-01	5.34-01	6.56-01	7.90-01	9.38-01	1.10-00	5.64
2300	6.78-02	1.42-01	2.23-01	3.11-01	4.08-01	5.14-01	6.30-01	7.57-01	8.96-01	1.05-00	5.38
2400	6.64-02	1.39-01	2.17-01	3.03-01	3.86-01	4.97-01	6.09-01	7.28-01	8.60-01	1.00-00	5.17
2500	6.52-02	1.36-01	2.12-01	2.95-01	3.65-01	4.69-01	5.89-01	7.05-01	8.30-01	9.67-01	4.96
2600	6.44-02	1.34-01	2.09-01	2.90-01	3.77-01	4.72-01	5.74-01	6.85-01	8.06-01	9.36-01	4.77
2700	6.37-02	1.32-01	2.06-01	2.85-01	3.71-01	4.63-01	5.62-01	6.70-01	7.86-01	9.12-01	4.59
2800	6.33-02	1.31-01	2.04-01	2.82-01	3.66-01	4.56-01	5.53-01	6.57-01	7.70-01	8.92-01	4.43
2900	6.30-02	1.30-01	2.02-01	2.78-01	3.62-01	4.51-01	5.46-01	6.48-01	7.58-01	8.76-01	4.28
3000	6.29-02	1.30-01	2.02-01	2.78-01	3.60-01	4.47-01	5.41-01	6.41-01	7.48-01	8.64-01	4.13
3100	6.30-02	1.30-01	2.01-01	2.77-01	3.58-01	4.45-01	5.37-01	6.36-01	7.41-01	8.54-01	4.00
3200	6.32-02	1.30-01	2.01-01	2.77-01	3.58-01	4.43-01	5.35-01	6.32-01	7.36-01	8.48-01	3.87
3300	6.35-02	1.31-01	2.02-01	2.78-01	3.58-01	4.43-01	5.34-01	6.30-01	7.33-01	8.43-01	3.76
4000	5.81-02	1.20-01	1.86-01	2.56-01	3.32-01	4.12-01	4.98-01	5.90-01	6.89-01	7.94-01	3.10
5000	5.76-02	1.18-01	1.81-01	2.47-01	3.16-01	3.89-01	4.65-01	5.45-01	6.29-01	7.17-01	2.48
6000	6.01-02	1.22-01	1.87-01	2.54-01	3.23-01	3.94-01	4.69-01	5.46-01	6.25-01	7.06-01	2.07
7000	6.63-02	1.33-01	2.03-01	2.77-01	3.52-01	4.28-01	5.07-01	5.89-01	6.73-01	7.60-01	1.77
8000	7.64-02	1.55-01	2.35-01	3.18-01	4.03-01	4.90-01	5.78-01	6.71-01	7.66-01	8.63-01	1.55
9000	9.04-02	1.83-01	2.78-01	3.75-01	4.75-01	5.78-01	6.83-01	7.91-01	9.01-01	1.02-00	1.38
10000	1.08-01	2.19-01	3.33-01	4.49-01	5.69-01	6.91-01	8.16-01	9.45-01	1.08-00	1.21-00	1.24

Photon Energy E(eV)	Net Density, D (Specular, 0.1 x 0.1 N.A.)										Wavelength λ(Å)
	0.2	0.4	0.6	0.8	1.0	1.2	1.4	1.6	1.8	2.0	
1000	3.03-01	6.87-01	1.17-00	1.79-00	2.56-00	3.55-00	4.79-00	6.37-00	8.37-00	1.09-01	12.40
1050	2.63-01	5.90-01	0.94-01	1.49-00	2.12-00	2.89-00	3.84-00	5.03-00	6.50-00	8.34-00	11.81
1100	2.33-01	5.16-01	0.60-01	1.28-00	1.79-00	2.41-00	3.17-00	4.10-00	5.23-00	6.61-00	11.27
1150	2.09-01	4.58-01	0.39-01	1.12-00	1.55-00	2.07-00	2.69-00	3.44-00	4.34-00	5.43-00	10.78
1200	1.90-01	4.15-01	0.61-01	0.96-01	1.37-00	1.81-00	2.33-00	2.96-00	3.70-00	4.58-00	10.33
1250	1.75-01	3.80-01	0.80-01	0.90-01	1.23-00	1.61-00	2.08-00	2.59-00	3.22-00	3.95-00	9.92
1300	1.63-01	3.52-01	0.57-01	0.70-01	1.12-00	1.46-00	1.85-00	2.31-00	2.85-00	3.48-00	9.54
1350	1.53-01	3.29-01	0.30-01	0.61-01	1.03-00	1.33-00	1.69-00	2.08-00	2.56-00	3.11-00	9.18
1400	1.45-01	3.10-01	0.48-01	0.55-01	0.95-01	1.23-00	1.55-00	1.92-00	2.34-00	2.82-00	8.86
1450	1.38-01	2.95-01	0.41-01	0.47-01	0.80-01	1.16-00	1.45-00	1.78-00	2.16-00	2.60-00	8.55
1500	1.33-01	2.82-01	0.30-01	0.40-01	0.68-01	1.08-00	1.36-00	1.67-00	2.02-00	2.42-00	8.27
1600	1.01-01	2.13-01	0.39-01	0.47-01	0.79-01	1.12-01	1.41-00	1.73-00	2.10-00	2.49-00	6.89
1800	0.67-02	1.04-01	0.33-01	0.40-01	0.63-01	0.93-01	1.16-00	1.43-00	1.75-00	2.11-00	6.53
2000	0.41-02	0.86-01	0.13-01	0.13-01	0.20-01	0.28-01	0.37-01	0.46-01	0.55-01	0.64-01	6.20
2100	0.23-02	0.74-01	0.05-01	0.05-01	0.08-01	0.11-01	0.14-01	0.17-01	0.20-01	0.23-01	5.80
2200	0.13-02	0.61-01	0.01-01	0.01-01	0.02-01	0.03-01	0.04-01	0.05-01	0.06-01	0.07-01	5.64
2300	0.09-02	0.50-01	0.00-01	0.00-01	0.01-01	0.01-01	0.01-01	0.01-01	0.01-01	0.01-01	5.38
2400	0.11-02	0.48-01	0.00-01	0.00-01	0.01-01	0.01-01	0.01-01	0.01-01	0.01-01	0.01-01	5.17
2500	0.18-02	0.46-01	0.00-01	0.00-01	0.01-01	0.01-01	0.01-01	0.01-01	0.01-01	0.01-01	4.96
2600	0.29-02	0.44-01	0.03-01	0.03-01	0.04-01	0.05-01	0.06-01	0.07-01	0.08-01	0.09-01	4.77
2700	0.45-02	0.42-01	0.07-01	0.07-01	0.08-01	0.09-01	0.10-01	0.11-01	0.12-01	0.13-01	4.59
2800	0.64-02	0.40-01	0.13-01	0.13-01	0.14-01	0.15-01	0.16-01	0.17-01	0.18-01	0.19-01	4.43
2900	0.87-02	0.38-01	0.20-01	0.20-01	0.21-01	0.22-01	0.23-01	0.24-01	0.25-01	0.26-01	4.28
3000	1.01-01	0.36-01	0.28-01	0.28-01	0.29-01	0.30-01	0.31-01	0.32-01	0.33-01	0.34-01	4.13
3100	1.04-01	0.35-01	0.27-01	0.27-01	0.28-01	0.29-01	0.30-01	0.31-01	0.32-01	0.33-01	4.00
3200	1.08-01	0.34-01	0.26-01	0.26-01	0.27-01	0.28-01	0.29-01	0.30-01	0.31-01	0.32-01	3.87
3300	1.11-01	0.33-01	0.25-01	0.25-01	0.26-01	0.27-01	0.28-01	0.29-01	0.30-01	0.31-01	3.76
4000	0.94-02	0.26-01	0.20-01	0.20-01	0.21-01	0.22-01	0.23-01	0.24-01	0.25-01	0.26-01	3.10
5000	1.14-01	0.23-01	0.19-01	0.19-01	0.20-01	0.21-01	0.22-01	0.23-01	0.24-01	0.25-01	2.48
6000	1.53-01	0.18-01	0.14-01	0.14-01	0.15-01	0.16-01	0.17-01	0.18-01	0.19-01	0.20-01	2.07
7000	2.08-01	0.13-01	0.09-01	0.09-01	0.10-01	0.11-01	0.12-01	0.13-01	0.14-01	0.15-01	1.77
8000	2.79-01	0.08-01	0.05-01	0.05-01	0.06-01	0.07-01	0.08-01	0.09-01	0.10-01	0.11-01	1.55
9000	3.69-01	0.04-01	0.03-01	0.03-01	0.04-01	0.04-01	0.05-01	0.05-01	0.06-01	0.06-01	1.38
10000	4.77-01	0.01-01	0.01-01	0.01-01	0.01-01	0.01-01	0.01-01	0.01-01	0.01-01	0.01-01	1.24

ABSORPTION EDGES

E: Br-L_{3,2} (1553-1599 eV) F: Ag-L_{3,2} (3351-3526 eV)

region as based upon D-I data at only these energies. In order to estimate the relative response of this film at the higher photon energies (> 1000 eV) we then simply extrapolated into the next energy decade the low-energy results using our model relations. We now present a more accurate characterization of the SB-392 for the high photon energies (1000-10,000 eV) using a D-I experimental data base representative only of this energy region and applying the improved procedures for the parameterization of the model description as has been described in detail above (Sec. III) for the characterization of the complementary Kodak DEF.

Using the same calibration procedure as described above for the present work, we have added D-I data for the Cu-K α (8050 eV) x-radiation to the previously measured data presented in Ref. 3 for the photon energies, Cu-L α (930 eV) and Al-K α (1490 eV). These data are presented in Fig. 11 along with the predicted curves using the analytical single-emulsion model equation (5) that is based upon a parameterization determined as follows:

The emulsion-plus-base thickness of the SB-392 was micrometered to be 196 μm . Using PET-crystal-monochromatized Cu-K α radiation, the transmission for two layers of the film, τ_F , and of two layers of the base, τ_b , (with the emulsion removed) were measured to be 0.461 and 0.725 respectively. These transmissions are related to the emulsion and base thicknesses, T and t_b , as follows:

$$T = \frac{1}{\mu'} \ln \sqrt{\frac{\tau_b}{\tau_F}} \quad (12)$$

$$t_b = \frac{1}{\mu_b} \ln \sqrt{\frac{1}{\tau_b}} \quad (13)$$

Applying these equations for the two layers of the film and of the base the single-emulsion thickness, T , base thickness, t_b , and the volume fraction of the AgBr grains, V , were determined to be 11.3 μm , 183.8 μm and 0.20 respectively. (It is interesting to note that these values were determined by model fitting alone of the low photon energy data in Ref. 2 to be, for T and V , 10 μm and 0.2.) With these parameters and with an estimated film grain size, d , from SEM measurements of 1 μm , the model relation for the single-emulsion film (5) was least-squares fitted to the data sets presented in Fig. 11 to yield the following values of fitting parameters, a and b , and of the supercoat thickness, t_0 :

$$a = 0.545 \mu\text{m}^{-1}, \quad b = 1.39 \mu\text{m}^2 \quad \text{and} \quad t_0 = 1.0 \mu\text{m}$$

In Ref. 3 we had reported the measured ratios, D_s/D_d , (net specular density/net diffuse density) for the specular densities, $D_{0.1}$ and $D_{0.25}$ (measured with microdensitometer influx and efflux matched optics at N.A. values of 0.1 and 0.25). These measurements yield the conversion equations for SB-392,

$$D_{0.1}/D_d = 1.6 - 0.10 D_d \quad (14)$$

$$D_{0.25}/D_d = 1.2$$

and

$$D_{0.1}/D_{0.25} = 1.3 - 0.07 D_{0.25} \quad (15)$$

Using (14) we have converted the diffuse density, D-I data on SB-5 by Koppel and Boyle⁹ and present these also in Fig. 11. (Their development procedure was 5 min in RXR at 68 deg. with agitation as compared with ours at 6 min in RXR at 72 deg. with agitation.)

SB 392 Density vs Exposure

X Henke et al. (1986)

△ Koppel and Boyle (1981)

— Single-Emulsion Model

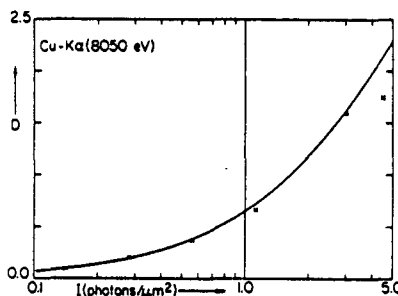
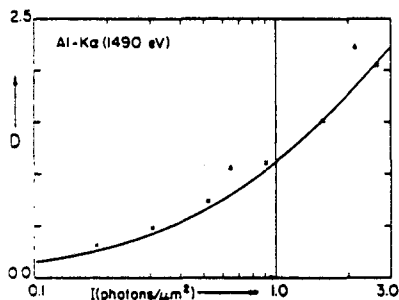
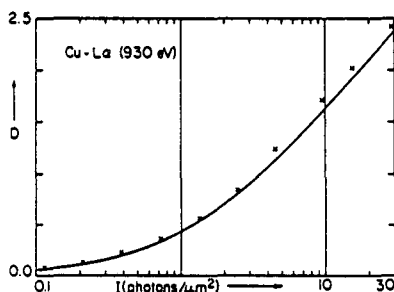


Fig. 11. The density-exposure data chosen here for the model equation fitting for SB-392 film at the representative photon energies, Cu-La (930 eV), Al-K α (1490 eV) and Cu-K (8050 eV). Also plotted here are the predicted D-I curves obtained by fitting the analytical model relation (5) to these total data. Optical densities are net densities (above unexposed, developed background density) as would be measured by using microdensitometry with matched influx and efflux optics of 0.1 N.A.

Using the analytical relation (5) thus determined for the SB-392 film, we presented in Fig. 10 its sensitivity, S, in comparison to that for DEF, and, in Table 2 we present the normal-incidence intensity, $I(\text{photons}/\mu\text{m}^2)$ that generates the specular density $D_{0.1}$ in the 0.2-2.0 range and at the photon energy $E(\text{eV})$ in the 1000-10,000 eV region.

Finally, it is important to note that for the single-emulsion film at medium or low exposures of sufficiently high photon energy x-radiation, the D-I relation becomes simply:

$$D = c\mu_1 I \quad (16)$$

with the energy dependence given completely as that for the absorption coefficient, μ_1 of AgBr and with the dependence upon the film grain size (before development) and the silver cluster grain size (after development) along with the T and V parameters disappearing within a single fitting parameter, c, which is independent of the angle of incidence, θ . This result may be readily derived by expanding the model relation (5) for the high energy limit for which $\mu_1 d$, $\mu_0 t_0$, and $\mu' T$ are small as compared with unity. For the Kodak SB-392 film exposed with medium or low intensities of photon energies around 10,000 eV, the D-I relation may be well approximated by the characteristic equation,

$$D_{0.1} = 7.3 \mu_1 (\mu\text{m}^{-1}) I(\text{photons}/\mu\text{m}^2) \quad (17)$$

where μ_1 is the linear absorption coefficient of AgBr for a particular photon energy (see μ_1 vs E table in Ref. 3).

V. SUMMARY

In this work we have presented detailed characterizations of the new, high sensitivity double-emulsion Kodak DEF film and the less sensitive but higher resolution single-emulsion Kodak SB-392 film for microdensitometric applications in the high energy x-ray region. These characterizations were shown not to be strongly affected by the normal variations (several laboratories evaluated) resulting from the choice of a conventional x-ray development procedures and from batch-to-batch differences. The accuracy of our averaging characterizations was mostly limited by the experimental errors of the D-I measurements. The magnitude of these errors and the accuracy of our characterizations may be estimated by the comparison of the D-I data from the several laboratories as plotted against our model curves in Figs. 5 and 11.

The three significant figures expressed in Tables 1 and 2 for the exposure, $I(\text{photons}/\mu\text{m}^2)$ are, of course, not indicative of the absolute accuracy of these averaged characterizations but rather of relative precision. The absolute accuracy can be evaluated and perhaps improved by fitting our average characterizations to a few experimental D-I film calibrations made on a particular film batch and with a given laboratory's measurement procedure.

The model relations that have been developed in this and the companion works^{2,3} for the response of x-ray films and presented here in (4) through (7) are relatively simple analytical relations amenable to small computer generation of absolute spectral intensities. These model descriptions are based upon two or three parameter fitting of a few D-I experimental data sets that are representative of the photon energy region of application. A simple procedure has been established for the determination of the basic geometric parameters of the x-ray film which are required for these model analytical descriptions.

The θ -dependence of our model relations (4) through (7) has been experimentally verified for incidence angles greater than about 10 degrees. (See Ref. 3) The same parameters that have been used to calculate the film characterizations presented in Tables 1 and 2 for normal incidence can be applied in these model equations to calculate the film response for smaller angles of incidence between 10 and 90 degrees.

In the Appendix we summarize a recommended film handling and processing procedure which will produce the DEF and SB-392 characteristics that have been described in this work.

ACKNOWLEDGEMENTS

The authors gratefully acknowledge the important assistance in this work of Debra Nanod, Ron Tackaberry and Jonathan Kerner, and the helpful suggestions of W.C. Phillips, G.N. Phillips, Jr. and of P.D. Rockett. This program on "Low Energy X-Ray Physics and Technology" at the University of California's Lawrence Berkeley Laboratory is supported by a grant from the Air Force Office of Scientific Research (AFOSR No. 84-0001) and supplementally by contracts with the Department of Energy (SAN#CID#9501, Task 1) via LANL and LLNL, and (No. DE-AC03-76SF00098) via LBL.

REFERENCES

1. B.L. Henke and P.A. Jaanimagi, "Two-Channel, Elliptical Analyzer Spectrograph for Absolute, Time-Resolving Time-Integrating Spectrometry of Pulsed X-Ray Sources in the 100-10,000 eV Region," *Rev. Sci. Instrum.* 56, 1537-1552 (1985).
2. B.L. Henke, S.L. Kwok, J.Y. Uejio, H.T. Yamada, and G.C. Young, "Low-Energy X-Ray Response of Photographic Films. I. Mathematical Models," *J. Opt. Soc. Am. B* 1, 818-827 (1984).
3. B.L. Henke, F.G. Fujiwara, M.A. Tester, C.H. Dittmore, and M.A. Palmer, "Low-Energy X-Ray Response of Photographic Films. II. Experimental Characterization," *J. Opt. Soc. Am. B* 1, 828-849 (1984).
4. W.C. Phillips and G.N. Phillips, Jr., "Two New X-Ray Films: Conditions for Optimum Development and Calibration of Response," *J. Appl. Cryst.* 18, 3-7 (1985).
5. P.D. Rockett, C.R. Bird, C.J. Hailey, D. Sullivan, D.B. Brown, and P.G. Burkhalter, "X-Ray Calibration of Kodak Direct Exposure Film," *Appl. Opt.* 24, 2536-2542 (1985).
6. B.L. Henke, H.T. Yamada and T.J. Tanaka, "Pulsed Plasma Source Spectrometry in the 80-8000-eV X-Ray Region," *Rev. Sci. Instrum.* 54, 1311-1330 (1983).
7. B.L. Henke, P. Lee, T.J. Tanaka, R.L. Shimabukuro, and B.K. Fujikawa, "Low-Energy X-Ray Interaction Coefficients: Photoabsorption, Scattering, and Reflection. E=100-2000 eV, Z=1-94," *At. Data Nucl. Data Tables* 27, 1-44 (1982).
8. The SEM film studies were kindly provided by David D. Dixon of the Technical Photography Group, Lawrence Livermore National Laboratory.
9. L.N. Koppel and M.J. Boyle, "X-Ray Calibration of Film Types SB-5 and RAR 2492 in the 1.5-8 keV Region," *Advanced Research and Applications Corp.*, Document No. FR-81-112-Sec. IV (1981).

APPENDIX : Film Handling and Development
Procedures

KODAK TYPE DEF (DEF-392)

The Kodak DEF or DEF-392 (the difference being the sheet film or 35 mm format) should be handled under Kodak Safelight Filter No. GBX-2 with a 15 watt bulb, no closer than 3 feet from the film. This practice should be followed during processing also. Special care should be taken not to bend the film too sharply, since doing so will result in many minute cracks in the emulsion. Fresh processing solutions should be used whenever possible, especially the developer, as it will deteriorate when in an open tray or processing tank. The processing of the film is as follows, with all solutions including the wash water at 68° F in either a developing tank for roll film or in a tray for sheet film:

1. Development: 5 min. in Kodak GBX developer, with gentle but continuous agitation
2. Rinse: 30 sec. in Kodak Indicator stop bath with gentle but constant agitation.
3. Fixing: 6 min. in Kodak Rapid Fixer or GBX fixer with constant agitation.
4. Wash: 30 min. in running water, then 30 sec. in Kodak Photo-Flo 200 working solution.
5. Drying: At room temperature in still air or at elevated temperatures, not over 100° F, in moving air.

In drying the film at elevated temperatures, care should be taken not to allow the relative humidity at the film to drop below 50%, as this can cause excessive shrinkage of the emulsion and a possible distortion of the image. The use of the Photo-Flo wetting agent will help promote uniform drying of the film by either method, with a minimum of drying artifacts and water spots.

Kodak Type SB-5 (SB-392)

Recommended film handling and development procedure is that described above for Kodak DEF.

This report was done with support from the Department of Energy. Any conclusions or opinions expressed in this report represent solely those of the author(s) and not necessarily those of The Regents of the University of California, the Lawrence Berkeley Laboratory or the Department of Energy.

Reference to a company or product name does not imply approval or recommendation of the product by the University of California or the U.S. Department of Energy to the exclusion of others that may be suitable.

*LAWRENCE BERKELEY LABORATORY
TECHNICAL INFORMATION DEPARTMENT
UNIVERSITY OF CALIFORNIA
BERKELEY, CALIFORNIA 94720*